INTEGRATED METHOD OF BUILDING EXTRACTION FROM DIGITAL SURFACE MODEL AND IMAGERY

Yan Li[1,] *, Lin Zhu[2], Hideki Shimamura[2],

[1] International Institute for Earth System Science, Nanjing University, Nanjing, Jiangsu, China, 210093, -liyan@nju.edu.cn
[2] PASCO Corporation, 1-1-2 Higashiyama, Meguro-ku, Tokyo, 153-0043, Japan

KEYWORD: Airborne remote sensing, Digital Surface Model, building, Feature extraction, Algorithms, Segmentation, Image

ABSTRACT:

In urban GIS and management, Digital surface model (DSM) can be used for generating object models. The preliminary step is to segment the interesting areas. In this paper, we present an integrated method of building extraction using transform from DSM to normal angles and watershed segmentation to the gradient of DSM. To remove the effect of the terrain shape to building detection, we firstly derive DTM from DSM by geomorphology filtering, and then generate Normalized DSM (NDSM) by subtracting DTM from DSM. Then the buildings can be extracted from NDSM. Since urban appearance is complicated with large buildings, small buildings, and woods, etc., building extraction is implemented through several stages. In the first stage, Local Surface Normal Angle Transformation (LSNAT) is implemented to DSM to extract lant roof buildings. In the second stage, Marker based watershed is implemented to get the boundaries of the objects above the ground. The result of marker based buildings and LSNAT based buildings are merged to improve the building extraction accuracy. At last, the orthogonal imagery is used to remove the woods according to the green color principle. A case study is implemented to a DSM of a region of Kounan, Japan with spatial resolution of 1m.

1. INTRODUCTION

Earth observing technologies have been developed for tens years. Sensors with more and more high spatial resolution have been developed and used in space borne and air borne remote sensing systems. The data acquired by these sensors has been used in a large amount of fields, especially in urban remote sensing, for example, urban modeling, and change detection, etc. Among these applications, building extraction and modeling become one of the most interested subjects as a fundamental of many other processes and analysis. The data source for this goal can be imagery, DSM acquired from laser or by photogrammetry, sometimes 2D GIS data, or the mixture of them (Brenner, 2000), (Ameri, 2000). Accordingly, there are techniques for extracting building from image (Rau et al. 2004, Suveg et al. 2002), and from Digital surface model (DSM) acquired from LIDAR point clouds data or laser data (Dell'Acqua, et al. 2001, Rottensteiner et al. 2002, Vosselman et al. 2001, TAN et al. 2002) or from image(Li et al. 2005, You et al. 2003), or sometimes both(Nakagawa et al. 2002, Chen et al. 2004).

In this research, we use DSM and imagery to detect and segment buildings and remove the trees.

Thus our interest focuses on the techniques of building detection from DSM. For that purpose, the points of the DSM have to be classified according to whether they belong to the terrain, to buildings or to other object classes, e.g., vegetation.(Rottensteiner et al. 2002**)**.

Unfortunately, in our effort to classify the vegetation from the building, we found it is difficult to get a satisfying result. Therefore, we decide not using DSM derived feature to partition the vegetation from the building, but color feature based on the imagery.

In this paper, we will describe an integrated approach of building extraction using transform from DSM to normal angles and watershed segmentation to the gradient of DSM. For this, we have taken several steps on DTM and NDSM generation, local surface normal angle transform (LSNAT) to extract buildings (for which we refer the normal based buildings), marker controlled watershed segmentation to extract the buildings (for which we refer the marker-watershed based buildings), and imagery based woods removal.

2. METHOD INTRODUCTION

2.1 DTM and NDSM Generation

The various heights of terrain will effect the building extraction, especially when height threshold can not be avoided. Thus DTM and normalized DSM (NDSM) are necessary for building extraction.

There are generally two ways to extract DTM from DSM. One is to detect buildings firstly and to exclude them from DSM. The other is to filter the DSM. We used morphological operators to remove the buildings from DSM because morphologic operations have been proved to be suitable for such shape processing of the objects. The morphological filter performs first a *close* operation to DSM to fill the pits in the DSM. After then, an *open* operation is performed to remove the surface obtrusions such as buildings, shrubs, and cars. Removing the above ground features in large scale element caused step effects on the DTM. To overcome this problem, a low pass filter is used to smooth the DTM. Figure 1 shows the DTM generation result from a DSM of Kounan, Japan. (a) is the source DSM, and (b) is smoothed DTM by lowpass filter. It can be seen that, general above ground features are removed and extra large buildings have their heights obviously decreased.

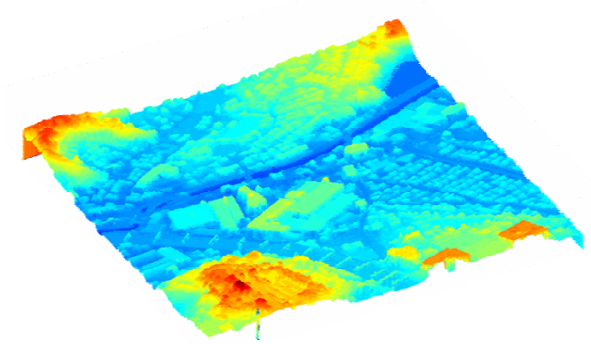

(a) DSM: md132-6 past dsm.

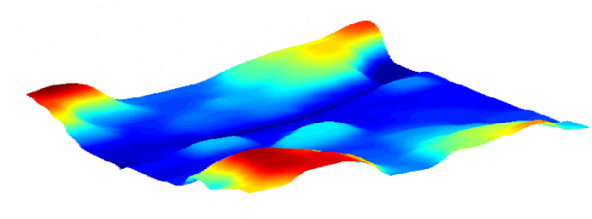

(b) Morphological filtered and low passed DTM of (a).
Figure 1 DSM and DTM

The system error and random error are represented by mean and standard deviation of DSM and terrain and DTM. We compared 7 patches basically of the ground or road randomly selected from DSM with the same ones of DTM in terms of the mean and the standard deviation. Table 1 shows the average heights of these patches for DSM and DTM and their differences. It is founded that the mean of DSM and DTM are very close for these patches. The greatest error is 4.2912, which is 1.3176m of height, the minimal error is 0.1864, which is 0.0572m, and the average error is 1.4479 which is 0.0046m of height.

Table 1 The mean of DSM terrain and DTM lowpassed							
Patch No.	1	2	3	4	5	6	7
DSM	73.205	78.701	63.532	67.642	122.431	56	81.179
DTM	68.914	79.919	63.264	66	121.297	55.814	79.782
difference	4.2912	-1.218	0.2672	1.642	1.134	0.1864	1.3968

Table 1 The mean of DSM terrain and DTM lowpassed

Because the DSM and DTM are available now, the NDSM is obtained by directly subtracting DTM from DSM here.

2.2 Local Surface Normal Angle Transform

A DSM can be visualized as a 3D surface, and the building roofs refer to the planar higher then the ground with certain spatial directions. We can extract these planar by retrieving the parameters of the local normal, and calculating the distributions of them and then extracting the peaks of the distributions.

There are several methods to fitting the normal to the surface using the location samples of the surface. Singular Value Decomposition (SVD) is used here to retrieve the normal vector. After that we transform the normal into 2 angles of α and β.

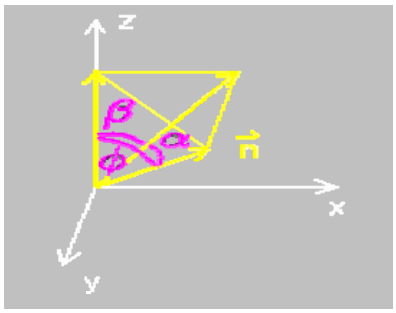

Figure 2 the normal vector and the relevant angles.

$$\alpha = sin^{-1}(n_2) \quad (1)$$

$$\beta = tg^{-1}\frac{n_1}{n_3} \quad (2)$$

Where n_1, n_2, n_3 refers to the weight of the unit normal in the three dimensions.

From the example map we can find that there are generally three colors in this DSM. It means that the directions of the normal vectors focus on these three directions. Thus we can extract these three directions from the 2D histogram of α and β, and then extract the associated pixels.

Figure 3(a) is the histogram of α and β for the above DSM and (b) is the binary one.

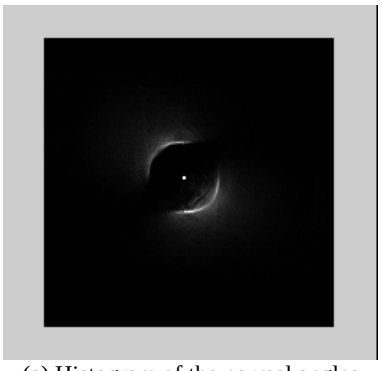

(a) Histogram of the normal angles

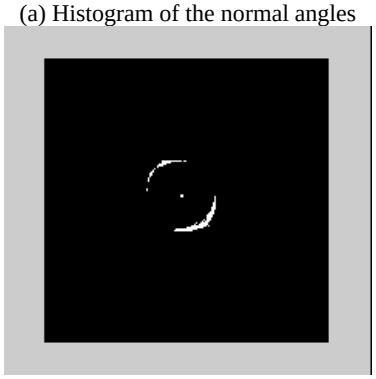

(b) Binary thresholded histogram

Figure 3

From Figure 3 we find that the two peaks are arcs with radius *r* and symmetric to the center peak. This relationship can be written as

$$\alpha^2 + \beta^2 = r^2 \tag{3}$$

Observing the relations of the triangle projected by the normal (n_1, n_2, n_3) to x-y plane in Figure 2, we can find that

$$\left(ztg\phi\right)^2 = \left(ztg\beta\right)^2 + \left(\frac{ztg\alpha}{\cos\beta}\right)^2 \tag{4}$$

It derives

$$\frac{\sin^2\phi}{1-\sin^2\phi} = \frac{\sin^2\beta}{1-\sin^2\beta} + \frac{\sin^2\alpha}{(1-\sin^2\alpha)(1-\sin^2\beta)} \tag{5}$$

If these angles are small (which are the practice) then the above equation can be approximated as

$$\frac{\phi^2}{1-\phi^2} = \frac{\beta^2}{1-\beta^2} + \frac{\alpha^2}{(1-\alpha^2)(1-\beta^2)} \tag{6}$$

Then we have

$$\phi^2 = \beta^2 + \alpha^2 - \beta^2\alpha^2 \tag{7}$$

It is further approximated as

$$\phi^2 = \beta^2 + \alpha^2 \tag{8}$$

This explains the relation of α and β. The radius r in Figure 3 is actually the angle ϕ.It means that the roofs have similar declining angles, ϕ, to the z-axis. The symmetric arcs in the histogram imply that the roofs are in two main declining angles which are symmetric to z-axis.

2.3 Marker Controlled Watershed Segmentation

2.3.1 Principle Introduction: Watershed to gray level image is suitable for the gray level images to separate the objects each others. But it will not give the actual boundaries of each object. Watershed to gradient image can resolve this problem. However, in practice, this transform produces an important over-segmentation due to noise or local irregularities in the gradient image. To avoid the over-segmentation, a marker controlled watershed is introduced (Gao *et al*. 2001, Salembier *et al*. 1994). By marker each object and the background, and make them the catchment bases, the desired objects can be acquired.

2.3.2 Foreground Markers: Buildings, trees, and so on which are above the ground are taken as the foreground objects and are assigned the foreground markers. There will be as many objects as foreground markers. This is the point of the method. The foreground marker is defined as the local maxima.

In practice, most of the roof, especially in the center, will be detected as the marker. For some objects, because they have not only one obstruction in the roof, there will be several markers detected and consequently they will be segmented as several objects.

Like in the method of normal based building extraction, to avoid multi-marker of the woods and huge buildings, large region is defined and detected. If not, there will be several catchment bases detected for one such region and therefore several objects with shrinking contours.

2.3.3 Background Markers: Because the watershed line of NDSM generally locate between objects, it is taken as the marker of background. Sometimes the background marker crosses the large regions so that these objects will merged in the background. A refine procedure is implemented to maintain these foreground markers. For example,

2.3.4 Marker Controlled Watershed: The procedure of Marker based watershed is described as following.

1, Impose the marker including the foreground markers and background marker to the GNDSM which is non negative to get the segmentation function G'. That it, make the locations of marker as -1 so that they are the local minima of G', or the catchment basin.

2, Implement watershed segmentation to G'.

2.3.5 Objects Above The Ground: Marker watershed segmentation is implemented to the gradient of NDSM, noted as GNDSM. The results we get are the objects with closed edges, where the maximum area one must be the ground. We assign the ground object as 0, just same with the edges between the objects, and the remained objects from 1 to O are the objects above the ground.

Recall of the large regions firstly get in the former step, the large regions are added in the objects by marker watershed.
At last, the orthogonal image is used to calculate the average green degree of all the objects. If the average levels for RGB channels are lower than certain values respectively, then the object is taken as the wood.

3. CASE STUDY

We have made experiments to evaluate the performance of our method. The DSM we used for experiments is in Kounan, Japan. The resolution of DSM is 1 meter and that of the image is 0.2 meter. We have made building extraction for three DSM. The sizes of them are listed in the second row in Table 2. Figure 4 shows the gray level map of one patch indexed by 134-2 of the DSM. There are more than one thousand houses in this region. Most of them are small ones neighboring closely each other.

Some of them can not even be separated by observing. There are also somewhere of woods, and houses within or near them. This is a challenge for the extraction of these buildings. The buildings extracted are shown in Figure 5.

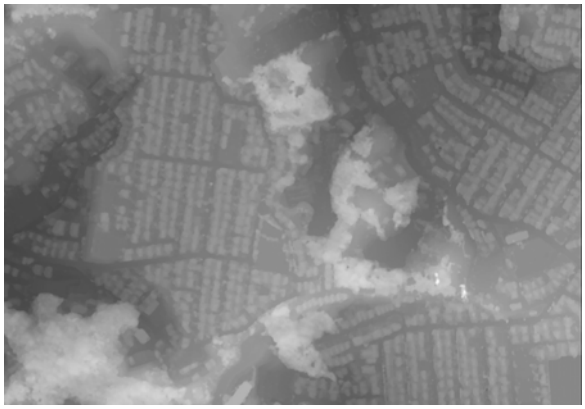

Figure 4 DSM of 134-2

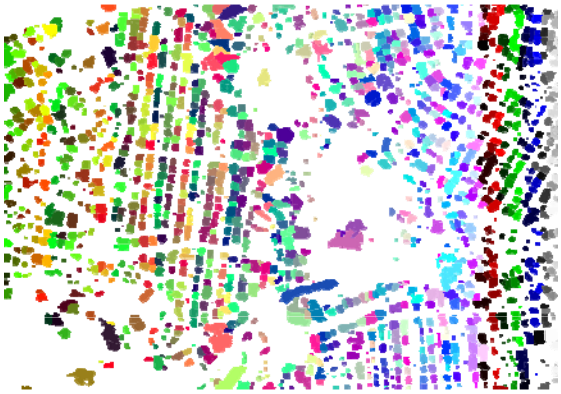

Figure 5 The last buildings result.

The detection accuracies of three DSM samples are displayed in the following form. This is done by compare the building extracted with the reference RGB image manually.

Table 2 detection accuracy analysis			
DSM No.	134-2	134-3	134-4
size	1125×1621	1145×1694	1151×1625
Building number	1108	957	1531
Building detected	1090	950	1523
Building missed	18	7	8
Detected accuracy （%）	98.38	99.27	99.48

Table 2 detection accuracy analysis

The detection performance can be evaluated by the definitions of good detection and bad detection. For good detection, we refer to the buildings in the RGB image that have corresponding detected buildings in the DSM. For bad detection, there are several cases.

1__ Building missing:

a> In NDSM, the missed buildings are connected with other ones with higher heights, so that they have no local maximal and thus no markers as foregrounds.

b> The buildings which are located between trees and are detected as large regions together with these trees, so that they will most likely be deleted as tree mass objects.

2__ Building mixing:

a> Taken as detected buildings.

b> There are no separate local maximal for these neighboring buildings but only one large local maximal due to their connected roof ridges.
c> Some buildings are taken as large regions.

3__ Building splitting

a> Taken as detected buildings.

b> There are several obstructions for such building so that several local maximal are detected as foreground markers and a building is detected as multiple ones.

4__ Building shrinking

a> Taken as detected buildings.

b> A high obstruction occurs above a building, and detected as a marker of the building, so that the maximum gradient pixels locate at the edges of the obstruction not the building boundaries.

REFERENCES

Ameri, B., 2000, Automatic recognition and 3D reconstruction of buildings from digital imagery. PhD Thesis, Institute of Photogrammetry, Stuttgart University, DGK-C 526.

Brunn, A., Weidner, U., 1997, Extracting Buildings from Digital Surface Models. IAPRS 32 (3-4W2), pp. 27-34.

Chen L.C., Teo T.A., Shao Y.C., Lai Y.C., and Rau J.Y., 2004, Fusion of LIDAR data and optical imagery for building modeling, Available online at: www.isprs.org/istanbul2004/comm4/papers/445.pdf

Dell'Acqua F., Gamba P., and Mainardi A., 2001, Digital terrain models in dense urban areas, International Archives of Photogrammetry and Remote Sensing, Volume XXXIV-3/W4, 22–24, October, 2001, Annapolis, MD,

Gao H.,Siu W.C. , and Hou C.H.. 2001, Improved techniques for automatic image segmentation, IEEE Transactions on Circuits and Systems for video technology, 11(12), 1273 - 1280.

Ibrahim S., Feature extraction and 3d city modeling using airborne lidar and high-resolution digital orthophotos, GIS Masters Thesis, The University of Texas at Dallas, Available online at: http://charlotte.utdallas.edu/mgis/prj_mstrs/2005/Fall/Ibrahim/Sulafa%20Ibrahim_MastersWebsite_Fall2005/LIDARAnalystDTMExtraction.htm

Li Y., Gong P., and Babu MB., 2005, Automated 3D building geometrical modeling from DSM, Proceedings of International Symposium on Spatio-temporal Modeling, Spatial Reasoning,

Spatial Analysis, Data Mining and Data Fusion, August 27-29, 2005, Beijing, China. pp.203-206,

Nakagawa M., Shibasaki R., and Kagawa Y., 2002, Fusing stereo linear CCD image and laser range data for building 3D urban model, Symposium on geospatial theory, processing and applications, ISPRS. Commission IV, WG IV7, July 9-12, 2002, Ottawa, Canada.

Rau, J.Y., Chen L.Q., and Wang G.H., 2004, An interactive scheme for building modeling using the split-merge-shape algorithm, Available online at: www.isprs.org/istanbul2004/comm3/papers/336.pdf

Rottensteiner, F. and Briese, C., 2002, A new method for building extraction in urban areas from high-resolution LIDAR data. IAPSIS XXXIV/3A (2002) 295–301.

Rottensteiner F., and Jansa J., 2002, Automatic extraction of buildings from lidar data and aerial images，Proceedings of the ISPRS Technical Commission IV Symposium 2002, IAPRS, Vol. XXXIV, part 4, ISSN 1682-1750.

Salembier P , and Pardas M., 1994, Hierarchical morphological segmentation for image sequence coding, IEEE Trans on Image Processing , 3 (5), 639 - 651.

Suveg I., and Vosselman G., 2002, Automatic 3D building reconstruction, Three-Dimensional Image Capture and Applications V, Brian D. Corner, Roy P. Pargas, Joseph H. Nurre, Editors, Proceedings of SPIE Vol. 4661 (2002)

Tan G., Shibasaki R., 2002, A research for the extraction of 3d urban building by using airborne laser scanner data, Available online at: www.gisdevelopment.net/aars/acrs/2002/urb/151.pdf

Vosselman, G., and Dijkman, S., 2001, 3D building model reconstruction from point clouds and ground plans. IAPSIS XXXIV(3W4) (2001) 37–43.

You H., and Li S., 2003, Building extraction from DSM acquired by airborne 3D image, Geospatial Information Science, 6, 25-31.